The Journal of Chemical Physics ARTICLE scitation.org/journal/jcp

A mean-field model of linker-mediated colloidal interactions

Cite as: J. Chem. Phys. 153, 124901 (2020); doi: 10.1063/5.0020578
Submitted: 2 July 2020 • Accepted: 31 August 2020 •
Published Online: 22 September 2020

W. Benjamin Rogers[a)]

AFFILIATIONS

Martin A. Fisher School of Physics, Brandeis University, Waltham, Massachusetts, 02453, USA

Note: This paper is part of the JCP Emerging Investigators Special Collection.
[a)]**Author to whom correspondence should be addressed:** wrogers@brandeis.edu. **URL:** www.rogers-lab.com

ABSTRACT

Programmable self-assembly is one of the most promising strategies for making ensembles of nanostructures from synthetic components. Yet, predicting the phase behavior that emerges from a complex mixture of many interacting species is difficult, and designing such a system to exhibit a prescribed behavior is even more challenging. In this article, I develop a mean-field model for predicting linker-mediated interactions between DNA-coated colloids, in which the interactions are encoded in DNA molecules dispersed in solution instead of in molecules grafted to particles' surfaces. As I show, encoding interactions in the sequences of free DNA oligomers leads to new behavior, such as a reentrant melting transition and a temperature-independent binding free energy per k_BT. This unique phase behavior results from a per-bridge binding free energy that is a nonlinear function of the temperature and a nonmonotonic function of the linker concentration, owing to subtle entropic contributions. To facilitate the design of experiments, I also develop two scaling limits of the full model that can be used to select the DNA sequences and linker concentrations needed to program a specific behavior or favor the formation of a prescribed target structure. These results could ultimately enable the programming and tuning of hundreds of mutual interactions by designing cocktails of linker sequences, thus pushing the field toward the original goal of programmable self-assembly: these user-prescribed structures can be assembled from complex mixtures of building blocks through the rational design of their interactions.

I. INTRODUCTION

Inspired by nature's ability to make complex structures and machines, self-assembly has emerged as a powerful technique for synthesizing nanoscale materials.[1–4] DNA-coated colloids provide a particularly promising approach since the base sequences grafted to particles can be designed to encode the formation of a chosen structure.[5–7] Although significant progress has been made in programming one or two colloidal species to form a variety of crystal lattices,[8–17] prescribing the myriad interactions required to assemble fully addressable, aperiodic structures remains an unsolved challenge[18–22] [Fig. 1(a)].

The most common scheme for DNA-programmed self-assembly relies on direct hybridization, in which particles bind to one another via complementary sequences grafted to their surfaces. Hybridization of complementary sequences induces a specific attraction that depends on the sequence, the coating density, the temperature, and the solution conditions[23–25] [Fig. 1(b)]. Because the attraction results from the combined molecular recognition and hybridization of grafted molecules, each specific pair interaction requires the design of a unique, orthogonal sequence. Therefore, creating a matrix of M specific interactions requires the design of M orthogonal sequences—one per pair interaction.

An alternative paradigm uses DNA oligomers dispersed in solution to encode the full matrix of pair interactions. In the simplest realization, each particle species is coated with a single sequence of DNA, and those sequences are designed to be non-complementary: The particles do not assemble on their own. Instead, all pair interactions are encoded in free DNA oligomers that "link" the particles together[17,26–28] [Fig. 1(c)]. Each linker sequence is comprised of two domains: one that binds to particle i and another that binds to particle j. Therefore, the binding of a linker L_{ij} will induce an attractive

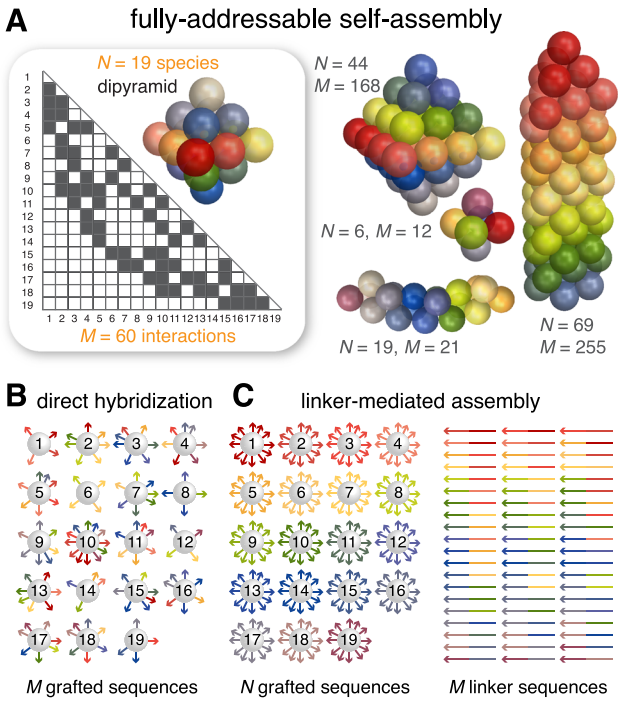

FIG. 1. (a) Fully addressable assembly involves encoding a matrix of M favorable interactions (gray) between N particle species. The renderings show example structures. Specific interactions are encoded in DNA sequences, which can be grafted to particles (b) or dispersed in solution (c). Programming linker-mediated assembly requires models to relate the linker sequences and concentrations to the pair interactions.

interaction between particles i and j. Thus, specifying a complex matrix of interactions in a mixture of many particle species can be accomplished by creating a library of linker sequences. Importantly, the matrix of interactions, and thus the free-energy landscape governing self-assembly, can be altered simply by changing the linker mixture.[17,28]

Realizing this vision of linker-programmed assembly requires simple models to design the linker sequences as well as their concentrations. In this article, I develop a mean-field model of linker-mediated binding using statistical mechanics and the principle of local chemical equilibrium. I show that the linker-based paradigm has a number of interesting features, such as a re-entrant melting transition and a temperature-independent binding free energy per k_BT, as compared to direct hybridization. I explain these new features by examining the per-bridge free energy and develop two scaling predictions that enable the rapid design of experiments by providing expressions for determining the binding free energy as a function of linker sequence and concentration. These simple rules, combined with the other advantages of linker-mediated binding, make linker-mediated assembly significantly easier to program than existing strategies. This new design flexibility could ultimately enable new directions in the fully addressable assembly of colloids.

II. A SIMPLE MODEL

I derive an approximate analytic model of linker-mediated attractions by extending an experimentally validated approach based on the principle of local chemical equilibrium. The original model was derived for the case of direct hybridization in the presence of additional displacer oligomers dispersed in solution, which could bind to compete with the grafted strands.[12] Here, I extend the model to describe linker-mediated binding in two steps: (1) I consider the partition function of two interacting particles and apply a mean-field approximation to estimate the probability that two particles are unbound as a function of the separation distance between them, and (2) I compute the unbound probability by treating DNA hybridization as a chemical reaction and using a local chemical equilibrium approach. The utility of the model that results is that it can predict the pair binding free energy between DNA-coated colloids from experimental inputs, such as the DNA coating density, the particle size, the DNA sequences, and the linker concentration. I focus on calculating the pair interaction potential, as opposed to calculating an equation of state directly,[29,30] with an eye toward future applications in fully addressable assembly of aperiodic structures,[18,31] like those illustrated in Fig. 1.

A. Mean-field description of DNA-induced interactions

I first relate the binding free energy between colloidal particles to the thermodynamics of hybridization in solution. The attractive free energy difference ΔF_a between a pair of particles that can be linked together by DNA bridges and a reference system in which the particles cannot bind is given by

$$\frac{\Delta F_a}{k_BT} = \ln P_{\text{unbound}}, \tag{1}$$

where P_{unbound} is the probability that there are no bridges linking the particles together.[23,24] P_{unbound} can be approximated by assuming that bridges are statistically independent and that the probability that a bridge has formed is given by the mean-field hybridization yield.[32] The hybridization yield χ can be calculated using the principles of mass-action, assuming that chemical equilibrium is established locally at each position $\mathbf{r}$.[12,33] In general, the hybridization yield depends on the position $\mathbf{r}$ because the sticky ends of the grafted molecules are highly localized near the particle surface (see the supplementary material for details).

For simplicity, I assume that the sticky ends are uniformly distributed within a spherical shell and consider only the interparticle separation distance that maximizes the overlap between the DNA shells. In general, the sticky-end concentrations can be generated numerically[24] by modeling the tethered DNA molecules as ideal chains of the known contour length and persistence length.[34] However, this approach prevents the derivation of an analytic expression for the pair free energy. Instead, I treat the sticky-end concentrations as uniform distributions with a local DNA concentration of $C_{i0} = \rho_{\text{DNA},i}/(N_{av}\delta)$, where $\rho_{\text{DNA},i}$ is the areal DNA grafting density of sequence i, N_{av} is Avogadro's number, and δ is the thickness of the DNA coating (Fig. 2). Under this additional simplifying assumption,[35] the binding free energy reduces to

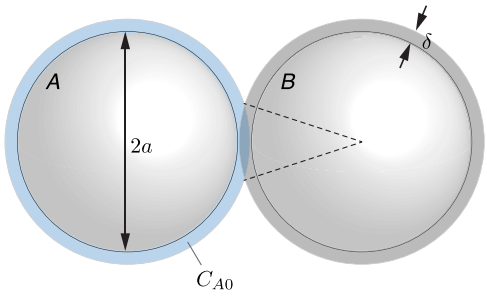

FIG. 2. A schematic of the two-sphere system. Colloidal particles of radius a are coated with single-stranded DNA with a local concentration C_{i0}, where i is the species type (either A or B). The DNA coating has an approximate thickness δ. Complementary DNA molecules can bind together in the contact region between two neighboring spheres. The maximum number of bridges that can form N_b is determined by the area of contact between two particles $A_{\text{contact}} \approx \pi a\delta$ and the limiting grafting density ρ_{DNA}.

$$\frac{\Delta F_a}{k_B T} \approx N_b \ln\left[1 - \chi(T)\right], \tag{2}$$

where $N_b \approx \pi a \delta \rho_{\text{DNA},A}$ is the maximum number of bridges that can form and a is the particle radius. Because N_b is the maximum number of bridges that can form, it is defined in terms of the lower of the two grafting densities. By convention, I take the lower grafting density to be sequence A.

For all calculations that follow, I use values that are representative of typical experiments in DNA-programmed colloidal self-assembly. More specifically, I use $\rho_{\text{DNA}} = 12{,}200/\mu\text{m}^2$, $\delta = 15$ nm, and $a = 500$ nm and compute the binding free energy when the particles are spaced apart by a distance δ. This DNA density and particle size were shown in experiment to result in the formation of equilibrium structures, namely, colloidal crystals.[13] I choose $\delta = 15$ nm since it is roughly the average end-to-end distance of typical single-stranded DNA molecules attached to the surface of a colloidal particle, which tend to range from 50 to 70 nucleotides in length.[13,23,24]

B. DNA hybridization as a chemical reaction network

Hybridization of complementary DNA sequences A, B, and L_{ab} can be modeled as a system of elementary chemical reactions

$$A + L_{ab} \overset{K_{eq}^{AL}}{\rightleftharpoons} AL_{ab},$$
$$B + L_{ab} \overset{K_{eq}^{BL}}{\rightleftharpoons} BL_{ab},$$
$$AL_{ab} + B \overset{K_{eq}^{BL}}{\rightleftharpoons} AL_{ab}B,$$
$$A + BL_{ab} \overset{K_{eq}^{AL}}{\rightleftharpoons} AL_{ab}B.$$

Here, A and B are the sequences grafted to particles, and L_{ab} is the linker sequence that binds A to B. The linker can adopt three conformations [Fig. 3(a)]: (1) it can be free in solution, L_{ab}; (2) it can form a "half-bridge," in which the linker is bound to a single grafted strand, AL_{ab} or BL_{ab}; or (3) it can form a "bridge," in which the linker connects together both A and B, $AL_{ab}B$.

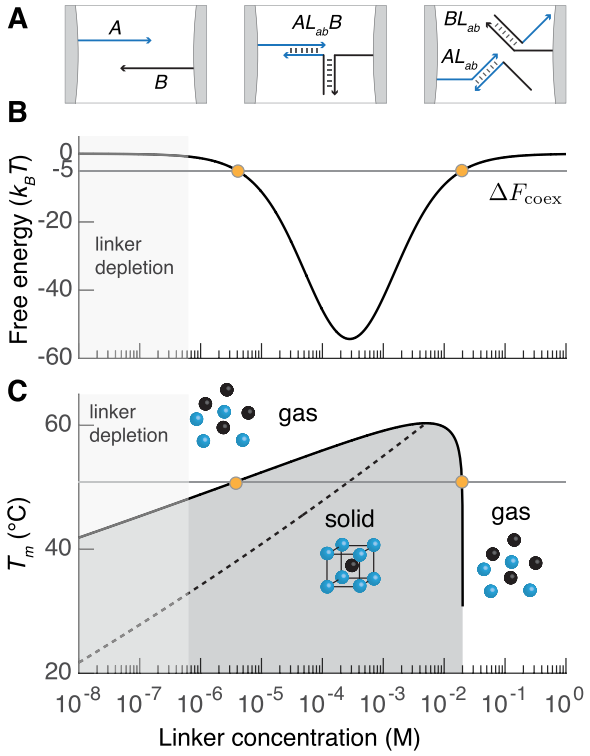

FIG. 3. Linker-mediated binding. (a) Molecular-scale reactions between grafted sequences A and B and linker sequence L_{ab} give rise to an effective binding free energy. (b) Predictions of the mean-field model (curve)—described in the text—show that the binding free energy is a non-monotonic function of the linker concentration. The horizontal line indicates the binding free energy at coexistence between gas and solid: ΔF_{coex}. The gray shaded region shows linker concentrations at which the assumptions of the model will break down. (c) The corresponding phase behavior exhibits a re-entrant melting transition. The solid curve shows predictions of the melting temperature as a function of linker concentration as described in the text. The dashed line shows the linker concentration corresponding to the maximum interaction strength for each temperature. The orange circles correspond to the coexistence temperatures between gas and solid. Model predictions are for $\Delta H° = -66.4$ kcal/mol, $\Delta S° = 0.1886$ kcal/mol K, $\rho_{\text{DNA}} = 12{,}200/\mu\text{m}^2$, and $b = 1$. The temperature in (b) is 51 °C. These thermodynamic parameters correspond to the 10-nt binding sequence 5′-TATGTGGTTA-3′.

The hybridization yield χ can be evaluated analytically assuming that linkers are not depleted from solution when they bind to the grafted strands. Taking the starting concentrations of A, B, and L_{ab} to be C_{A0}, $C_{B0} = bC_{A0}$, and $C_{L_{ab}0}$, where $b \geq 1$, the hybridization yield $\chi = C_{AL_{ab}B}/C_{A0}$ can be evaluated by solving the system of equations describing the equilibrium constants of each elementary reaction, as well as the mole balances of each DNA species A, B, and L_{ab}. When $C_{L_{ab}} \approx C_{L_{ab}0}$, the hybridization yield is given by

$$\chi = \frac{(b+1)K'_{eq} + 1 - \sqrt{(b-1)^2(K'_{eq})^2 + 2(b+1)K'_{eq} + 1}}{2K'_{eq}}, \tag{3}$$

where K'_{eq} is a concentration-adjusted equilibrium constant (see the supplementary material for details).

The hybridization yield depends only on a single parameter: a concentration-adjusted free energy change. I define the concentration-adjusted free energy change to be $\Delta G'/RT = -\ln K'_{eq}$, yielding

$$\frac{\Delta G'}{RT} = -\ln\left[\frac{K_{eq}^{AL}K_{eq}^{BL}\frac{C_{A0}C_{L_{ab}0}}{(C^\circ)^2}}{\left(1+K_{eq}^{AL}\frac{C_{L_{ab}0}}{C^\circ}\right)\left(1+K_{eq}^{BL}\frac{C_{L_{ab}0}}{C^\circ}\right)}\right], \tag{4}$$

where C_{i0} is the initial concentration of species i, $C^\circ = 1$ M is a reference concentration, $K_{eq}^{i}(T) = \exp[-\beta\Delta G_i(T)]$ is the equilibrium constant, $1/\beta$ is the thermal energy k_BT, and $\Delta G_i = \Delta H_i - T\Delta S_i$ is the standard free energy difference between products and reactants at the reference concentration C°.

Interestingly, the concentration-adjusted free energy change $\Delta G'$ has a nontrivial functional dependence. For instance, whereas the free energy change of hybridization in solution ΔG_i has a linear dependence on the temperature, the temperature dependence of $\Delta G'$, which enters via the equilibrium constants, is nonlinear. The concentration-adjusted free energy change also has a complex dependence on the linker concentration since $C_{L_{ab}0}$ appears in both the numerator and denominator. Therefore, on the basis of the expression for $\Delta G'$ alone, we anticipate that linker-mediated interactions might have a few tricks up their sleeve, as we will see shortly.

The assumption that linkers are not depleted upon bridge formation is valid in the limit in which the linkers L_{ab} are in large stoichiometric excess compared to the grafted strands A and B. It turns out that this condition is satisfied for a wide range of parameter values. Because the grafted strands are confined within a spherical shell of volume $4\pi a^2\delta$, linkers are in stoichiometric excess when $C_{L_{ab}0} > 3\rho_{\mathrm{DNA},i}\phi_0/(N_{av}a)$, where ϕ_0 is the initial colloid volume fraction. For a typical volume fraction of $\phi_0 = 0.01$, this threshold linker concentration corresponds to roughly $C_{L_{ab}0} = 600$ nM. Above this value, the system contains more linkers than grafted DNA molecules. Thus, I assume that the linkers are not depleted for all calculations that follow.

III. RESULTS AND DISCUSSION

A. Non-monotonic binding free energy

The predicted binding free energy is a non-monotonic function of the linker concentration. Figure 3(b) shows predictions of the binding free energy as a function of increasing linker concentration at fixed temperature. The binding free energy is roughly zero for the lowest linker concentrations explored: 10 nM–100 nM. As the linker concentration increases, the binding free energy becomes more and more negative until linker concentrations of about 200 μM–300 μM. At even higher linker concentrations, the binding free energy turns around and increases upon increasing linker concentration until it approaches 0 k_BT again at around 100 mM. This non-monotonic dependence of the binding free energy on linker concentration is qualitatively different than the behavior observed in the direct binding case. There, increasing the density of grafted DNA strands always increases the strength of attraction.[25]

The non-monotonic nature of the binding free energy arises from the molecular-scale reactions between DNA molecules. At the lowest linker concentrations, there are too few linkers to stabilize bridges between particles. Thus, the particles cannot bind. At intermediate concentrations, adding additional linkers shifts the equilibrium of the elementary DNA reactions toward the bridged configuration $AL_{ab}B$, increasing the strength of attraction. At even higher linker concentrations, the system switches to favor the formation of half-bridges AL_{ab} and BL_{ab}, effectively passivating the particles against binding. Because both the bridged conformation $AL_{ab}B$ and two half-bridged conformations AL_{ab} and BL_{ab} have the same number and type of base pairs, the balance between these two regimes is determined entirely by entropy. I return to this point in Sec. III C. It is also worth noting that the minimum in the free energy occurs at a linker concentration that is more than two orders of magnitude higher than the stoichiometric amount. This observation suggests that the non-monotonic nature of the binding free energy is more subtle than one might first expect.

The model predictions show that the binding free energy can be tuned over a wide range of values by adjusting the linker concentration for a fixed suspension of particles. Over the range of linker concentrations in which the model should be accurate—above roughly 500 nM—the interactions can be tuned from 0 k_BT to almost −60 k_BT by changing the linker concentration by about two orders of magnitude [Fig. 3(b)]. This ability to tune the binding free energy has a number of potential uses within programmable self-assembly: (1) A colloidal suspension can be directed toward equilibrium structures, such as crystals, by making the interactions weak and reversible,[12,13,15] or toward non-equilibrium structures, such as gels and clusters, by making the interactions much stronger than k_BT,[36–38] (2) the pair interactions in a complex mixture of many particle species can be matched to one another by tweaking the relative concentrations of the linker species, thereby increasing or decreasing the binding free energy to account for small differences in the hybridization free energies between DNA sequences,[18,39] and (3) the same suspension can be steered toward different assemblies by adjusting the relative binding free energies, and thus the underlying free-energy landscape, via the linker concentrations.[17]

B. The phase behavior

A direct consequence of the non-monotonic binding free energy is a generic phase diagram with a re-entrant melting transition back to the gas phase at high linker concentrations. I predict the phase behavior that emerges from linker-mediated binding by using the mean-field model to find the coexistence temperature between gas and solid. I model the gas as an ideal gas and the solid using a simple cell model,[40] in which I approximate the potential as a square-well with depth ΔF_a and range δ. Equating the chemical potential of the gas to the chemical potential of the solid yields an expression for the pair free energy at coexistence $\Delta F_{\mathrm{coex}}/k_BT = [\ln(\rho v_f) + 1]/(Z/2)$, where Z is the coordination number of the solid phase, $v_f = (\delta/2)^3$ is the volume available to a particle within the solid phase, $\rho = \phi/(4/3\pi a^3)$ is the equilibrium density of the gas phase, and ϕ is the equilibrium volume fraction of the gas phase. By analogy to hybridization of DNA strands in solution, I define the melting temperature to be the temperature at which half of the particles remain in the gas phase $\phi = \phi_0/2$. Therefore, choosing $Z = 8$

and $\phi_0 = 0.01$—typical values for assembly of the binary cesium chloride crystal lattice[17]—yields a binding free energy at coexistence of roughly $\Delta F_{coex} \approx -5\ k_B T$. I stress that the conclusions presented below do not depend strongly on these choices. Indeed, adjusting Z or ϕ_0 slightly produces only modest changes in the binding free energy at coexistence.

The generic phase diagram has a concentration-dependent melting temperature and a re-entrant transition to the gas phase at high linker concentrations. Upon increasing linker concentration, the melting temperature increases logarithmically: The melting temperature changes from roughly 40 °C to 60 °C upon increasing the linker concentration from roughly 10 nM to 1 mM, about five orders of magnitude in concentration [Fig. 3(c)]. Upon increasing the linker concentration further by only about a factor of two to three, the melting temperature plummets and the system returns to the gas phase. This generic phase behavior matches previously reported experimental results.[28] Within the context of programmable self-assembly, one lesson is that there exists a finite range of linker concentrations over which particles will assemble.

Although the model also makes predictions at the lowest linker concentrations, these predictions are expected to be inaccurate given that a central assumption of the model—that linkers are not depleted—will break down. The interactions here should be modeled using more complete theories,[28] but these approaches are beyond the scope of this article. More importantly, the region where the model breaks down is also the region where the system is expected to be kinetically arrested. More specifically, because the melting temperature is lower for low linker concentrations, the off rates of DNA hybridization are also correspondingly slower.[17,41,42] As demonstrated by Pine and co-workers, slow off rates can hinder local rearrangements within a growing assembly, thereby suppressing crystallization.[13] Thus, the lowest linker concentrations are unlikely to be used in equilibrium assembly experiments, such as the formation of prescribed aperiodic packings of spheres or crystallization of ordered lattices.

C. Concentration-adjusted free energy

Examining the concentration-adjusted free-energy difference sheds light on the origin of the re-entrant melting transition and suggests that the thermodynamics of binding is governed by two limiting behaviors. Figure 4 shows the dependence of $\Delta G'/RT$ on temperature for a range of linker concentrations $C_{L_{ab}0}$. Unlike hybridization in solution,[43] the concentration-adjusted free energy change is a nonlinear function of temperature. It decreases linearly with decreasing temperature at high temperatures and then plateaus at low temperatures. I call these two regimes "limit 1" and "limit 2." Furthermore, the transition between the two limits, as well as the magnitude of the plateau, depends on the linker concentration: The transition shifts to higher temperatures, and the plateau increases in magnitude for increasing linker concentration. These two trends are independent of the specific linker sequence.

The concentration-dependent melting temperature and the re-entrant melting transition originate from the concentration-adjusted free-energy difference. I define $\Delta G'_{coex}$ to be the concentration-adjusted free energy change at melting. Upon increasing linker concentration, the temperature at which $\Delta G'$ crosses the melting threshold increases (Fig. 4). Again, this

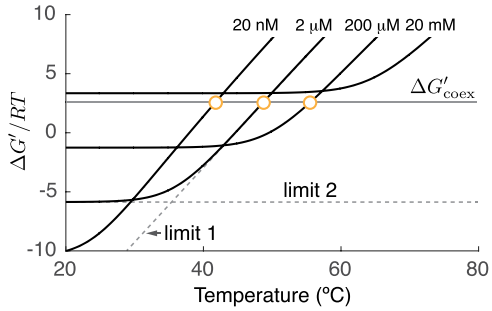

FIG. 4. The unique linker-mediated phase behavior arises from the concentration-adjusted free energy. Solid curves show model predictions of $\Delta G'$ as a function of temperature for four linker concentrations: 10 nM, 1 μM, 100 μM, and 1 mM. $\Delta G'/RT$ shows two limiting behaviors: (1) It decreases linearly with decreasing temperature at high temperatures, and (2) it becomes independent of temperature at low temperatures. I call these two limits "limit 1" and "limit 2," respectively. The orange circles correspond to the coexistence temperatures between gas and solid. Model predictions are for $\Delta H° = -66.4$ kcal/mol, $\Delta S° = 0.1886$ kcal/mol K, $\rho_{DNA} = 12{,}200/\mu m^2$, and $b = 1$.

observation is due to the fact that increasing the linker concentration shifts the equilibrium toward bridged conformations. However, because increasing linker concentration also increases the magnitude of the plateau, eventually there exists a linker concentration for which $\Delta G'$ never crosses $\Delta G'_{coex}$ (Fig. 4): The system transitions to a new regime and cannot aggregate for any of the linker concentrations above this value. This point is precisely the condition defining the re-entrant melting transition. Importantly, we can see that both phenomena originate entirely from the concentration-adjusted free energy change, and thus both are equilibrium effects.

Finally, I highlight one more interesting feature of linker-mediated binding: that the binding free energy saturates at low temperatures rather than decreasing monotonically, as expected for direct hybridization. Because $\Delta G'/RT$ plateaus at low temperature, the binding free energy per $k_B T$, $\Delta F_a/k_B T$, must also plateau at low temperatures since its sole temperature dependence arises from K'_{eq}. As a result, the binding free energy per $k_B T$ becomes temperature-independent at low temperatures. This observation is reminiscent of previous results reported for DNA-coated colloids interacting with displacing strands dispersed in solution.[12] Indeed the mechanisms are the same. The temperature independence of the interactions arises from a competition between two states with the same number of base pairs and thus the same enthalpy: One state links the particles together, and the other state does not. In the linker case, these two states are (1) the bridged state $AL_{ab}B$ and (2) the fully half-bridged state AL_{ab} and BL_{ab}. Since the enthalpies of these two states are equal, their relative thermodynamic stability depends entirely on entropy, which is controlled by the linker concentration. A similar prediction was reported recently for linker-mediated binding of DNA-coated colloids whose grafted DNA molecules are fluid and can diffuse on the surface of the colloidal particles.[44] This softening of the temperature dependence for linker-mediated binding might help to facilitate equilibrium assembly of DNA-coated colloids since it could limit kinetic trapping that results from the steep nature of the temperature-dependent interactions.[25,45]

D. Scaling predictions

I next develop two scaling limits to further explore the origin of the unique phase behavior, as well as to aid in the design of linker sequences and their mutual concentrations for future experiments in addressable self-assembly. Because typical equilibrium experiments probe conditions in which colloidal interactions are weak, I assume that the hybridization yield χ is small and only a small number of the total available bridges form in equilibrium. This limit is equivalent to taking $K'_{eq} \to 0$, which yields a simplified expression for the binding free energy:

$$\frac{\Delta F_a}{k_B T} \approx -bN_b K'_{eq}. \tag{5}$$

Owing to the non-monotonic nature of the concentration-adjusted free energy change $\Delta G'$, and thus the concentration-adjusted equilibrium constant K'_{eq}, there are two further limits that can be evaluated: (1) a high-temperature limit in which bridge formation is governed by the binding of free linkers from solution ("limit 1") and (2) a low-temperature limit in which bridge formation is governed by a competition between full bridges and half-bridges ("limit 2"). Although somewhat counter intuitive, it is important to notice that binding between colloids can be weak ($K'_{eq} \ll 1$) even when binding between complementary DNA molecules is strong ($K^i_{eq} \gg 1$), again due to the competition between hybridized states (see the supplementary material for details).

1. Limit 1: Concentration-dependent interactions

The high-temperature limit tells us about the concentration dependence of the melting transition. Taking the limit in which $K^i_{eq} C_{L_{ab}0}/C^\circ \ll 1$, the binding free energy reduces to

$$\frac{\Delta F_a}{k_B T} = -\pi a \delta^2 N_{av} K^{AL}_{eq} K^{BL}_{eq} \frac{bC^2_{A0} C_{L_{ab}0}}{(C^\circ)^2}. \tag{6}$$

Here, the binding free energy is a linear function of the linker concentration and the equilibrium constants of the two half–bridge reactions K^i_{eq}.

The predictions of this scaling result match predictions from the full model when the binding free energy is weak. Figure 5 shows a comparison between the melting temperature predicted from the full model [Eq. (2)] and the melting temperature predicted by the scaling limit [Eq. (6)] for different linker concentrations, grafting densities, and linker sequences. These predictions collapse to a single curve, which falls nearly along $y = x$, indicating that the scaling limit captures the essential physics near the melting transition. The fact that the scaling limit slightly overestimates the melting temperature likely results from the assumption that the hybridization yield χ is very small. In practice, the hybridization yield at the melting transition will be finite for low grafting densities, which weakens the binding free energy, an effect captured by the full model.

Most importantly, the collapse of the scaling predictions shows that the melting temperature is determined by an equilibrium between free linkers and bridges, and that Eq. (6) can be used to accurately predict the binding free energies, given a set of linker sequences and concentrations. Indeed, all of the variables in Eq. (6) can be controlled, determined from experimental measurements, or predicted from the DNA sequences. For example, the particle size a and the linker concentration $C_{L_{ab}0}$ are specified by the experimenter; the DNA grafting density can be measured by flow cytometry;[13,23,24] and the equilibrium constants can be predicted from the DNA sequences using the nearest-neighbor model.[43] Therefore, for a given set of linker sequences, particle sizes, and grafting densities, Eq. (6) can be used to select linker concentrations that will target a user-specified melting temperature, at which an equilibrium self-assembly experiment can then be performed.

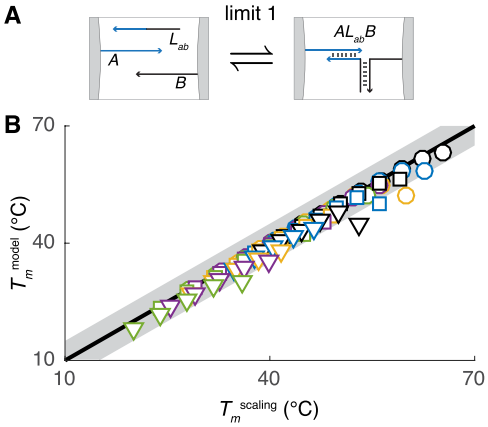

FIG. 5. Comparing predictions of the melting temperature from the full model and the scaling limit 1. (a) At high temperatures, bridge formation is dominated by hybridization of free linkers from solution. (b) Predictions of the melting temperature from the full model T_m^{model} vs predictions of the melting temperature from the scaling limit 1 T_m^{scaling} for different sequences, grafting densities, and linker concentrations. The color indicates the sticky-end length and thus hybridization free energy: 12 bp (black), 11 bp (blue), 10 bp (orange), 9 bp (purple), and 8 bp (green). The symbol type indicates the number of DNA molecules per particle: 10 000 (circle), 3000 (square), and 920 (triangle). The solid black line shows $y = x$, and the gray band shows a range of $T_m^{\text{model}} \pm 5°$C. Note that the linker is twice the length of the sticky end since the linker is comprised to two binding domains.

It is worth pointing out that the binding free energy within the high-temperature limit is similar to an earlier mean-field model due to Crocker and co-workers. Starting with the same two-sphere partition function, they showed that the binding free energy is simply the average number of bridges multiplied by the thermal energy, under conditions at when the hybridization yield χ is negligibly small:[23] $\Delta F_a/k_B T \approx -\chi N_b = -\langle N_b \rangle$. Assuming that bridges form exclusively via the molecular reaction $A + L_{ab} + B \rightleftharpoons AL_{ab}B$ [Fig. 5(a)], the hybridization yield is given by

$$\chi = K^{AL}_{eq} K^{BL}_{eq} \frac{bC_{A0} C_{L_{ab}0}}{(C^\circ)^2}. \tag{7}$$

Therefore, multiplying this expression for the hybridization yield χ by the number of potential bridges $N_b = \pi a \delta^2 N_{av} C_{A0}$ reproduces the result that we found in Eq. (6).

The final observation within the high-temperature limit is that the binding free energy is proportional to the equilibrium constants of the two half–bridge reactions and is thus an exponential function of the hybridization free energies. A direct consequence of

this dependence is that small differences in the hybridization free energies between DNA molecules are compounded into large differences in the binding free energy. Interestingly, this sensitivity to the hybridization free energies, and thus the DNA sequences,[43] should enhance the specificity of binding between DNA-coated colloids as compared to binding of complementary DNA molecules in solution.

With only a four-letter alphabet, we are all but guaranteed to have some undesired overlap between sequences in a complex mixture containing hundreds of unique linker species. The combinatorics of the sequence design space have been worked out by Wu *et al.*[46] They determined that the number of unique sequences of length N without any undesired overlaps longer than $M-1$ is given by $P = (4^M - 4^{M/2})/(2 \times (N - M + 1))$ if M is even. Therefore, if $N = 11$ and $M = 6$, there are $P = 336$ unique sequences that do not have 5 bp or longer off-target overlaps. A sticky-end sequence with 11 nucleotides (nt) is completely sensible within the model developed here. In fact, the blue symbols within Fig. 5 correspond to a sticky-end length of 11 nt. Therefore, it is possible to design a sufficient number of sequences to program the assembly of the structures in Fig. 1. However, do the sequence overlaps compromise the specificity of binding and thus undermine the premise of using linkers to program fully addressable assembly?

A simple back-of-the-envelope estimate suggests that off-target binding is insignificant. The average change in the Gibbs free energy per base pair upon hybridization is roughly −1.4 kcal/mol at 37 °C.[43] Therefore, the hybridization free energy of a full 11-bp complement is −15.4 kcal/mol, and the hybridization free energy of a 5-bp, off-target sequence is −7 kcal/mol. Consider the scenario in which one binding domain is complementary and the other domain has a 5-bp, off-target overlap. The relative binding free energies between this scenario and the fully complementary case, in which the linker forms all 22 base pairs, would be roughly 10^{-6}. The scenario in which both binding domains of a linker have 5-bp, off-target domains is even better. There, the relative binding free energies between the on-target and off-target sequences would be roughly 10^{-12}. Therefore, it seems plausible that the vast majority of the 336 unique linkers with 11-nt binding domains could be used to program the self-assembly of complex, prescribed structures.

2.Limit 2: Re-entrant melting

Whereas the high-temperature limit told us about the concentration dependence of the melting transition, the low-temperature limit tells us about the re-entrant transition to the gas phase. Taking the limit in which $K^i_{eq} C_{L_{ab}0}/C^\circ \gg 1$, the binding free energy reduces to

$$\frac{\Delta F_a}{k_B T} = -\pi a \delta^2 N_{av} \frac{b C_{A0}^2}{C_{L_{ab}0}} \tag{8}$$

(see the supplementary material for details).

Examining Eq. (8) highlights three unique features of the low-temperature limit: (1) The binding free energy per k_BT does not depend on the temperature nor the linker sequence since the equilibrium constants do not appear in the expression; (2) the binding free energy is proportional to the square of the grafting density; and (3) the binding free energy is inversely proportional to the linker concentration. In contrast to the behavior in limit 1, increasing the linker concentration within limit 2 *decreases* the binding free energy.

This new limiting behavior again arises from molecular-scale reactions. At low temperatures, the system will tend to maximize the number of base pairs to lower its energy. Therefore, bridge formation will be driven by a competition between half-bridged and bridged states since both have all possible bases paired. For example, Fig. 6(a) illustrates a molecular reaction whereby two half-bridged states AL_{ab} and BL_{ab} react to form a bridge plus a free linker. Assuming $\Delta G_{AL_{ab}B} = \Delta G_{AL_{ab}} + \Delta G_{BL_{ab}}$, the change in the hybridization free energy of this reaction is 0, explaining the absence of the equilibrium constants in Eq. (8). Furthermore, in the limit where the hybridization yield of bridges χ is small, yet the grafted strands are bound to linkers, the hybridization yield is given by

$$\chi = \frac{b C_{A0}}{C_{L_{ab}0}}. \tag{9}$$

Therefore, we can see that the right-hand side of Eq. (8) is again simply $-\langle N_b \rangle$, but now for the molecular reaction $AL_{ab} + BL_{ab} \rightleftharpoons AL_{ab}B + L_{ab}$ instead of for the reaction $A + L_{ab} + B \rightleftharpoons AL_{ab}B$ (see the supplementary material).

The predictions of the re-entrant concentration from the scaling limit match predictions from the full model at high grafting densities. Setting $\Delta F_a = \Delta F_{\text{coex}}$, Eq. (8) can be rearranged to find the linker concentration at the re-entrant melting transition, which I call the re-entrant concentration $C_{L_{ab}0,re}$. Figure 6(b) shows predictions of the re-entrant concentration from the full model [Eq. (2)]

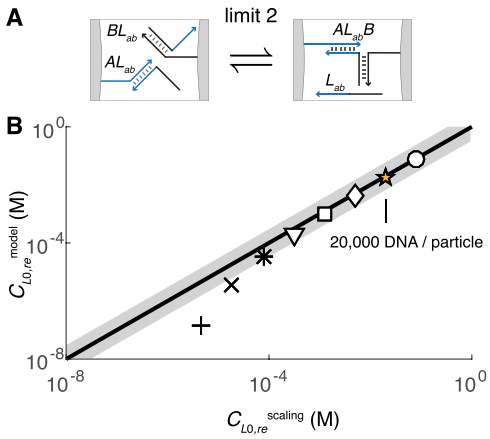

FIG. 6. Comparing predictions of the re-entrant linker concentration from the full model and the scaling limit 2. (a) At low temperatures, bridge formation is dominated by competition between half-bridged and full-bridged configurations. (b) Predictions of the re-entrant concentration from the full model $C_{L0,re}^{\text{model}}$ vs predictions of the re-entrant concentration from the scaling limit 2 $C_{L0,re}^{\text{scaling}}$ for different sequences and grafting densities. Predictions for different sequences overlap and cannot be differentiated. The symbol type indicates the number of DNA molecules per particle, increasing from 300 (+) to 38 400 (circle) by factors of two. The solid black line shows $y = x$, and the gray band shows a range of $C_{L0,re}^{\text{model}}$ multiplied or divided by a factor of three.

against predictions from the scaling limit [Eq. (8)] for different grafting densities. At high grafting densities, the full-model predictions match the scaling predictions (they fall along $y = x$). Predictions of the full model diverge from the scaling predictions at low grafting densities. Below grafting densities of roughly 2400 DNA molecules per 1-μm-diameter particle, the scaling prediction overestimates the re-entrant concentration. This deviation results from the fact that the extent of reaction required to induce assembly is finite and the simplifying assumption that $\ln(1 - \chi) \approx K'_{eq}$ is no longer accurate. However, the scaling predictions for densities typical of equilibrium assembly experiments—roughly 20 000 DNA molecules per 1-μm-diameter particle—are in excellent agreement with the predictions of the full model, showing that the scaling limit can again be used to design experiments.

The final observation within this limit concerns the squared dependence of the re-entrant concentration on the grafting density. One might be tempted to conclude that the re-entrant transition back to the fluid phase is a trivial consequence of there being more linkers in solution than grafted DNA molecules. A corollary of this explanation is that the re-entrant concentration would be directly proportional to the grafting density. The fact that the re-entrant concentration depends on the grafting density squared shows that this interpretation is incorrect. Moreover, returning to the predictions of the full model in Fig. 3(c), we can see that the re-entrant transition occurs only when there are 3–4 orders of magnitude more linkers in solution than grafted strands. The reason that the simple intuition fails is central to many problems in soft-matter physics: entropy. Whether or not the system prefers to link particles together to induce assembly or to passivate them to prevent binding depends on the entropy penalty associated with plucking a linker from solution and binding it to particles. As I have shown, capturing these subtleties and going beyond our intuition, which can be misleading when dealing with systems in which entropy plays a dominant role, requires a statistical-mechanical approach.

IV. CONCLUSIONS

In this work, I developed a simple mean-field model of linker-mediated interactions between colloids. Using this model, I showed that the interactions have a number of interesting features, such as a nonmonotonic dependence on the linker concentration, as well as a temperature-independent, strong-binding limit. I also developed two scaling limits, which agree well with the predictions of the full model when the binding free energy is comparable to k_BT. These two scaling limits provide convenient closed-form analytical expressions that can be used to design DNA sequences or select linker concentrations for future experiments in programmable self-assembly.

Whereas this paper focused specifically on linker-mediated interactions between DNA-coated colloids, the models developed herein could be used to describe other systems in which weak, multivalent binding is induced by free linkers dispersed in solution. The linkers could be divalent molecules, as considered here, or small colloidal particles with specific attractions that bridge large particles together. Indeed, a number of recent experimental and theoretical reports have explored various possibilities of using soluble linkers to control interactions and subsequent self-assembly of colloidal particles.[29,30,47–52] One feature that is common to all of these studies is a re-entrant transition to a fluid phase at high linker concentrations. Therefore, the re-entrant transition appears to be a generic feature of linker-mediated assembly.

One benefit of the model presented here is that it provides both a thermodynamic and a molecular-scale interpretation of the re-entrant transition. While earlier models also make predictions regarding the re-entrant transition, it is difficult to deduce the underlying mechanisms directly from the bulk phase behavior.[47,48,50] Because the core of our approach is a network of chemical reactions that leads to bridge formation, we can use the principles of chemical equilibrium and mass action to interpret the emergent binding free energy. For instance, we found that the re-entrant transition is governed by a reaction in which two half-bridges combine to form a bridge while simultaneously liberating a free linker. In other words, near the re-entrant transition, bridge formation is essentially a bimolecular chemical reaction. Therefore, we can think of the squared dependence of the binding free energy on the grafting density as arising simply from mass action: In dynamic equilibrium, the average number of bridges is proportional to the product of the two grafting densities. Similarly, we can understand the observation that the binding free energy gets weaker upon increasing linker concentration. This trend arises from the fact that a linker is liberated upon bridge formation. Therefore, adding additional linkers shifts the equilibrium away from the bridged state and thus weakens the binding free energy. In both cases, these effects are completely entropic.

Going forward, these findings may also open new possibilities for programming dissipative pathways to self-assembly. While this article described the utility of linker-mediated interactions for equilibrium assembly, there is growing interest in pursuing new non-equilibrium pathways as well. Because the sequences and concentrations of DNA oligomers dispersed in the solution can be easily modified *in situ*, the interaction matrix can, in principle, be programmed to vary in time and in space. For example, by creating more complex chemical reaction networks than those described above, it should be possible to integrate logic circuits,[53] biochemical oscillators,[54,55] all-or-none switches,[56,57] or reaction-diffusion patterns[58,59] into colloidal self-assembly. The incorporation of these types of dynamical systems into self-assembly could provide complementary pathways to programming more exotic materials than specificity alone.

SUPPLEMENTARY MATERIAL

A detailed development of the model is available in the supplementary material.

ACKNOWLEDGMENTS

I acknowledge Huang Fang, Janna Lowensohn, Bortolo M. Mognetti, and Rees Garmann for fruitful conversations. I also acknowledge financial support from the National Science Foundation (Grant No. NSF DMR-1710112), the Brandeis MRSEC (Grant Nos. NSF DMR-1420382 and NSF DMR-2011846), and the Smith Family Foundation.

DATA AVAILABILITY

The data that support the findings of this study are available from the corresponding author upon reasonable request.

REFERENCES

[1]G. M. Whitesides and B. Grzybowski, "Self-assembly at all scales," Science **295**, 2418–2421 (2002).
[2]S. C. Glotzer and M. J. Solomon, "Anisotropy of building blocks and their assembly into complex structures," Nat. Mater. **6**, 557–562 (2007).
[3]P. Yin, H. M. T. Choi, C. R. Calvert, and N. A. Pierce, "Programming biomolecular self-assembly pathways," Nature **451**, 318–322 (2008).
[4]L. Cademartiri and K. J. M. Bishop, "Programmable self-assembly," Nat. Mater. **14**, 2–9 (2015).
[5]M. R. Jones, N. C. Seeman, and C. A. Mirkin, "Programmable materials and the nature of the DNA bond," Science **347**, 1260901 (2015).
[6]W. B. Rogers, W. M. Shih, and V. N. Manoharan, "Using DNA to program the self-assembly of colloidal nanoparticles and microparticles," Nat. Rev. Mater. **1**, 16008 (2016).
[7]C. R. Laramy, M. N. O'Brien, and C. A. Mirkin, "Crystal engineering with DNA," Nat. Rev. Mater. **4**, 201–224 (2019).
[8]A. V. Tkachenko, "Morphological diversity of DNA-colloidal self-assembly," Phys. Rev. Lett. **89**, 148303 (2002).
[9]R. J. Macfarlane, B. Lee, M. R. Jones, N. Harris, G. C. Schatz, and C. A. Mirkin, "Nanoparticle superlattice engineering with DNA," Science **334**, 204–208 (2011).
[10]M. Casey, R. Scarlett, W. Rogers, I. Jenkins, T. Sinno, and J. Crocker, "Driving diffusionless transformations in colloidal crystals using DNA handshaking," Nat. Commun. **3**, 1209 (2012).
[11]Y. Zhang, F. Lu, K. G. Yager, D. Van Der Lelie, and O. Gang, "A general strategy for the DNA-mediated self-assembly of functional nanoparticles into heterogeneous systems," Nat. Nanotechnol. **8**, 865 (2013).
[12]W. B. Rogers and V. N. Manoharan, "Programming colloidal phase transitions with DNA strand displacement," Science **347**, 639–642 (2015).
[13]Y. Wang, Y. Wang, X. Zheng, É. Ducrot, J. S. Yodh, M. Weck, and D. J. Pine, "Crystallization of DNA-coated colloids," Nat. Commun. **6**, 7253 (2015).
[14]A. V. Tkachenko, "Generic phase diagram of binary superlattices," Proc. Natl. Acad. Sci. U. S. A. **113**, 10269–10274 (2016).
[15]Y. Wang, I. C. Jenkins, J. T. McGinley, T. Sinno, and J. C. Crocker, "Colloidal crystals with diamond symmetry at optical lengthscales," Nat. Commun. **8**, 14173 (2017).
[16]D. J. Lewis, L. Z. Zornberg, D. J. Carter, and R. J. Macfarlane, "Single-crystal winterbottom constructions of nanoparticle superlattices," Nat. Mater. **19**, 719–724 (2020).
[17]J. Lowensohn, A. Hensley, M. Perlow-Zelman, and W. B. Rogers, "Self-assembly and crystallization of DNA-coated colloids via linker-encoded interactions," Langmuir **25**, 7100–7108 (2020).
[18]Z. Zeravcic, V. N. Manoharan, and M. P. Brenner, "Size limits of self-assembled colloidal structures made using specific interactions," Proc. Natl. Acad. Sci. U. S. A. **111**, 15918–15923 (2014).
[19]Y. Ke, L. L. Ong, W. M. Shih, and P. Yin, "Three-dimensional structures self-assembled from DNA bricks," Science **338**, 1177–1183 (2012).
[20]W. M. Jacobs, A. Reinhardt, and D. Frenkel, "Rational design of self-assembly pathways for complex multicomponent structures," Proc. Natl. Acad. Sci. U. S. A. **112**, 6313–6318 (2015).
[21]W. M. Jacobs and D. Frenkel, "Self-assembly of structures with addressable complexity," J. Am. Chem. Soc. **138**, 2457–2467 (2016).
[22]L. L. Ong, N. Hanikel, O. K. Yaghi, C. Grun, M. T. Strauss, P. Bron, J. Lai-Kee-Him, F. Schueder, B. Wang, P. Wang *et al.*, "Programmable self-assembly of three-dimensional nanostructures from 10 000 unique components," Nature **552**, 72–77 (2017).
[23]P. L. Biancaniello, A. J. Kim, and J. C. Crocker, "Colloidal interactions and self-assembly using DNA hybridization," Phys. Rev. Lett. **94**, 058302 (2005).
[24]W. B. Rogers and J. C. Crocker, "Direct measurements of DNA-mediated colloidal interactions and their quantitative modeling," Proc. Natl. Acad. Sci. U. S. A. **108**, 15687–15692 (2011).
[25]R. Dreyfus, M. E. Leunissen, R. Sha, A. V. Tkachenko, N. C. Seeman, D. J. Pine, and P. M. Chaikin, "Simple quantitative model for the reversible association of DNA coated colloids," Phys. Rev. Lett. **102**, 048301 (2009).
[26]H. Xiong, D. van der Lelie, and O. Gang, "DNA linker-mediated crystallization of nanocolloids," J. Am. Chem. Soc. **130**, 2442–2443 (2008).
[27]H. Xiong, D. van der Lelie, and O. Gang, "Phase behavior of nanoparticles assembled by DNA linkers," Phys. Rev. Lett. **102**, 015504 (2009).
[28]J. Lowensohn, B. Oyarzún, G. N. Paliza, B. M. Mognetti, and W. B. Rogers, "Linker-mediated phase behavior of DNA-coated colloids," Phys. Rev. X **9**, 041054 (2019).
[29]B. A. Lindquist, R. B. Jadrich, D. J. Milliron, and T. M. Truskett, "On the formation of equilibrium gels via a macroscopic bond limitation," J. Chem. Phys. **145**, 074906 (2016).
[30]M. P. Howard, R. B. Jadrich, B. A. Lindquist, F. Khabaz, R. T. Bonnecaze, D. J. Milliron, and T. M. Truskett, "Structure and phase behavior of polymer-linked colloidal gels," J. Chem. Phys. **151**, 124901 (2019).
[31]J. D. Halverson and A. V. Tkachenko, "DNA-programmed mesoscopic architecture," Phys. Rev. E **87**, 062310 (2013).
[32]Note that this assumption does not require that the bridge distribution is a Poisson distribution.
[33]W. B. Rogers and J. C. Crocker, "Reply to Mognetti *et al.*: DNA handshaking interaction data are well described by mean-field and molecular models," Proc. Natl. Acad. Sci. U. S. A. **109**, E380 (2012).
[34]M. C. Murphy, I. Rasnik, W. Cheng, T. M. Lohman, and T. Ha, "Probing single-stranded DNA conformational flexibility using fluorescence spectroscopy," Biophys. J. **86**, 2530–2537 (2004).
[35]E. W. Gehrels, W. B. Rogers, and V. N. Manoharan, "Using DNA strand displacement to control interactions in DNA-grafted colloids," Soft Matter **14**, 969–984 (2018).
[36]M. E. Leunissen, R. Dreyfus, F. C. Cheong, D. G. Grier, R. Sha, N. C. Seeman, and P. M. Chaikin, "Switchable self-protected attractions in DNA-functionalized colloids," Nat. Mater. **8**, 590–595 (2009).
[37]N. B. Schade, M. C. Holmes-Cerfon, E. R. Chen, D. Aronzon, J. W. Collins, J. A. Fan, F. Capasso, and V. N. Manoharan, "Tetrahedral colloidal clusters from random parking of bidisperse spheres," Phys. Rev. Lett. **110**, 148303 (2013).
[38]L. Di Michele, F. Varrato, J. Kotar, S. H. Nathan, G. Foffi, and E. Eiser, "Multistep kinetic self-assembly of DNA-coated colloids," Nat. Commun. **4**, 2007 (2013).
[39]S. Hormoz and M. P. Brenner, "Design principles for self-assembly with short-range interactions," Proc. Natl. Acad. Sci. U. S. A. **108**, 5193–5198 (2011).
[40]P. Charbonneau and D. Frenkel, "Gas-solid coexistence of adhesive spheres," J. Chem. Phys. **126**, 196101 (2007).
[41]G. Bonnet, O. Krichevsky, and A. Libchaber, "Kinetics of conformational fluctuations in DNA hairpin-loops," Proc. Natl. Acad. Sci. U. S. A. **95**, 8602–8606 (1998).
[42]W. B. Rogers, T. Sinno, and J. C. Crocker, "Kinetics and non-exponential binding of DNA-coated colloids," Soft Matter **9**, 6412–6417 (2013).
[43]J. SantaLucia, Jr. and D. Hicks, "The thermodynamics of DNA structural motifs," Annu. Rev. Biophys. Biomol. Struct. **33**, 415–440 (2004).
[44]X. Xia, H. Hu, M. P. Ciamarra, and R. Ni, "Linker-mediated self-assembly of mobile DNA-coated colloids," Sci. Adv. **6**, eaaz6921 (2020).
[45]R. Dreyfus, M. E. Leunissen, R. Sha, A. Tkachenko, N. C. Seeman, D. J. Pine, and P. M. Chaikin, "Aggregation-disaggregation transition of DNA-coated colloids: Experiments and theory," Phys. Rev. E **81**, 041404 (2010).
[46]K.-T. Wu, L. Feng, R. Sha, R. Dreyfus, A. Y. Grosberg, N. C. Seeman, and P. M. Chaikin, "Polygamous particles," Proc. Natl. Acad. Sci. U. S. A. **109**, 18731–18736 (2012).
[47]C. Zhao, G. Yuan, D. Jia, and C. C. Han, "Macrogel induced by microgel: Bridging and depletion mechanisms," Soft Matter **8**, 7036–7043 (2012).
[48]J. Chen, S. R. Kline, and Y. Liu, "From the depletion attraction to the bridging attraction: The effect of solvent molecules on the effective colloidal interactions," J. Chem. Phys. **142**, 084904 (2015).

[49]L. Feng, B. Laderman, S. Sacanna, and P. Chaikin, "Re-entrant solidification in polymer–colloid mixtures as a consequence of competing entropic and enthalpic attractions," Nat. Mater. **14**, 61–65 (2015).
[50]J. Luo, G. Yuan, C. Zhao, C. C. Han, J. Chen, and Y. Liu, "Gelation of large hard particles with short-range attraction induced by bridging of small soft microgels," Soft Matter **11**, 2494–2503 (2015).
[51]E. Locatelli, P. H. Handle, C. N. Likos, F. Sciortino, and L. Rovigatti, "Condensation and demixing in solutions of DNA nanostars and their mixtures," ACS Nano **11**, 2094–2102 (2017).
[52]G. C. Antunes, C. S. Dias, M. M. Telo da Gama, and N. A. M. Araújo, "Optimal number of linkers per monomer in linker-mediated aggregation," Soft Matter **15**, 3712–3718 (2019).
[53]Y.-J. Chen, N. Dalchau, N. Srinivas, A. Phillips, L. Cardelli, D. Soloveichik, and G. Seelig, "Programmable chemical controllers made from DNA," Nat. Nanotechnol. **8**, 755 (2013).
[54]J. Kim and E. Winfree, "Synthetic *in vitro* transcriptional oscillators," Mol. Syst. Biol, **7**, 465 (2011).
[55]K. Montagne, R. Plasson, Y. Sakai, T. Fujii, and Y. Rondelez, "Programming an *in vitro* DNA oscillator using a molecular networking strategy," Mol. Syst. Biol. **7**, 466 (2011).
[56]J. Kim, K. S. White, and E. Winfree, "Construction of an *in vitro* bistable circuit from synthetic transcriptional switches," Mol. Syst. Biol. **2**, 68 (2006).
[57]A. Padirac, T. Fujii, and Y. Rondelez, "Bottom-up construction of *in vitro* switchable memories," Proc. Natl. Acad. Sci. U. S. A. **109**, E3212–E3220 (2012).
[58]J. Zenk, D. Scalise, K. Wang, P. Dorsey, J. Fern, A. Cruz, and R. Schulman, "Stable DNA-based reaction–diffusion patterns," RSC Adv. **7**, 18032–18040 (2017).
[59]G. Gines, A. S. Zadorin, J.-C. Galas, T. Fujii, A. Estevez-Torres, and Y. Rondelez, "Microscopic agents programmed by DNA circuits," Nat. Nanotechnol. **12**, 351 (2017).